

MONITORING NEUTRON FLUX USING

RECOIL ALPHA PARTICLES

Bertrand Bordet

A THESIS

in

The Department of

Physics

Presented in Partial Fulfilment of the Requirements for

the Degree of Master of Science at

Concordia University

Montreal, Canada

April, 1975

ABSTRACT

BERTRAND BORDET

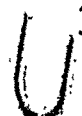

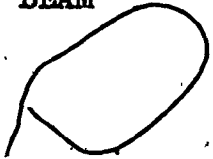
MONITORING NEUTRON FLUX USING RECOIL ALPHA PARTICLES

A computer program has been written to calculate the neutron flux produced by accelerated deuterons bombarding a tritium loaded titanium target (TiT_n). The experimental determination of this neutron flux from the reaction $H^3(d,n)He^4$ by the monitoring of the recoil alpha particles has been studied. An experimental comparison with the activation foil technique has been made using $Cu^{63}(n,2n)Cu^{62}$.

TABLE OF CONTENTS

	Page
ACKNOWLEDGEMENTS	i
LIST OF DIAGRAMS	ii
CHAPTER I INTRODUCTION	1
CHAPTER II INTERACTION OF HEAVY PARTICLES WITH MATTER	4
2.1 Generalities	4
2.2 Interaction of heavy charged particles with matter	4
2.3 Energy loss of a charged particle	5
2.4 Range of a charged particle	9
2.5 Interaction of neutrons with matter	11
CHAPTER III THEORETICAL DETERMINATION OF THE NEUTRON YIELD	14
3.1 Target characteristics	14
3.2 Nuclear Reactions	15
3.3 Method of calculation	16
CHAPTER IV EXPERIMENTAL DETERMINATION OF THE NEUTRON FLUX BY ALPHA MONITORING	21
4.1 Alpha Detection: Surface barrier detectors and alpha spectrum	21
4.2 Correction due to counting losses	26
4.3 Anisotropic correction factor	28
4.4 Geometrical factor	30
4.5 Losses due to a misfocused beam	35
4.6 Experimental results and calculations	37
4.7 Foil activation technique for measuring neutron yield	38

4.8	Conclusion	40
APPENDIX I	ERROR IN THE ANISOTROPIC FACTOR DUE TO THE COMPOSITION OF THE BEAM	43
APPENDIX II	PROGRAM. "NEUFLU"	45
REFERENCES		48



ACKNOWLEDGEMENTS

The author wishes to thank Dr. N. Eddy for his interest, guidance and constant encouragement during the course of the research.

LIST OF DIAGRAMS

Figure Number	Caption	Page
1	Charge particle scattering with electrons	6
2	Particle nuclear reaction with emission of two different particles.	
	(a) Laboratory coordinates	29
	(b) Center of mass coordinates	30
3	Energy spectrum for alpha particles going out of the target.	24
4	Schematic of typical surface barrier detector	25
5	Target assembly design	31
6	Geometry of a point source located on the center axis of a circular aperture.	32
7	Worst possible geometry condition for a point source located off target center	32
8	Cross section of beam normal to its direction. Beam out of focus by $\frac{1}{16}$	36

LIST OF TABLES

1	Deuterons: Statistics	12 13
2	Neutron flux in neutrons/second	20

CHAPTER IINTRODUCTION

Research laboratories, both academic and industrial, are more and more dependent on the precision of their quantitative analysis measurements. Among these precise measurements, trace element analysis is becoming a key factor of development in a large range of activities such as electronics, metallurgy, chemistry, biology, medicine etc... Different techniques are used to improve the determination of trace elements: mass spectroscopy, atomic absorption, spectrophotometry etc... One of the most sensitive and reliable is neutron activation analysis.

The general procedure followed by this technique is the following: The sample, the composition of which is to be determined, is bombarded by neutrons. These neutrons react with matter by colliding with nuclei present in the sample, thus initiating different nuclear reactions which are specific to the elements - more exactly, to the isotopes encountered in the sample.

The products of these reactions, mainly the gamma rays, are studied to determine qualitatively and quantitatively which isotopes are present in the sample.

Neutron activation analysis itself is divided into two different techniques according to the kinetic energy of the neutrons used to induce the nuclear reactions:

- (1) Neutron activation by slow (thermal) neutrons whose energy is below 1000 eV. Their main sources are nuclear reactors which produce large neutron fluxes ($10^{16} \text{ n cm}^{-2} \text{ s}^{-1}$) (1)

- (2) Neutron activation by fast neutrons whose energies are over 0.5 MeV. They may originate from α emitters mixed with beryllium, such as Ra(Be) or Pu(Be), or from nuclear reactions induced by accelerators.

This last procedure often uses 14 MeV neutrons obtained in a Cockcroft Walton generator in which accelerated deuterons react with tritium absorbed into a tungsten matrix with a copper backing. The reaction is



In this case, the precision of a quantitative analysis depends primarily on two factors a) the exact determination of the neutron flux and b) the precision of the values of the cross sections of the nuclear reaction used for the analysis. The object of this work is the determination of the neutron flux, first theoretically, for targets with different atomic ratios N and for incident deuterons with energies up to 200 keV, then experimentally by monitoring

the alpha particles associated with the neutron production.

The value of the neutron flux measured by the alpha monitoring technique has been compared to that obtained from foil activation in the same experiment.

CHAPTER IIINTERACTION OF HEAVY PARTICLES WITH MATTER2.1 Generalities:

Most of the experimental facts we are dealing with in this work are closely related to the interaction of particles with matter. Therefore a brief review of this theory is necessary to understand the following facts:

- The indirect determination of neutron flux by alpha monitoring
- The choice of neutrons for activation analysis.

2.2 Interaction of heavy charged particles with matter:

We are dealing with alpha particles and deuterons which interact mainly with the atomic electrons of the material for the following reasons:

1) Electrons are dispersed throughout a volume much larger than the volume occupied by the nuclei (size of atom $\approx 10^4$ x size of nucleus)

2) Deuterons and alpha particles are obliged to overcome the coulomb barrier before colliding with the nuclei.

Calculations from program NEUFLU (Appendix 2) show that the probability for a 200 keV deuteron reacting with 1.75 tritium atoms per titanium atom is only of the

order of 3×10^{-5} before this deuteron is stopped.

Collisions with Ti nuclei are practically impossible because of the large coulomb barrier of these nuclei.

In this case interaction with nuclei may be neglected.

The particle is considered as travelling in an electron gas, and the interaction of the charged particle with matter leads to collisions with atomic electrons in which either an electron is excited to a higher atomic quantum state (excitation of the atom); or the electron receives enough energy to leave the atom (ionization).

2.3 Energy loss of charged particle: (2)

Assumptions

1) Alpha particles and deuterons are much heavier than electrons; their deflection is very small and can be neglected, and their path is considered to be straight.

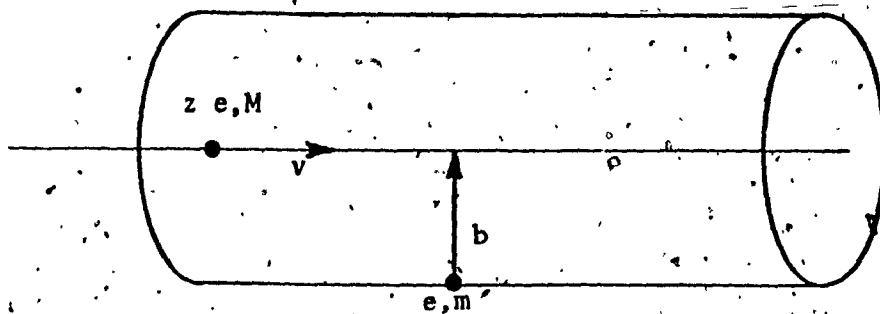
2) The maximum energy of the alpha particles encountered in our experiment is 3.58 MeV which means a velocity $\approx \frac{4.3}{100} C$ (C = velocity of light).

for the deuterons (200 keV), the velocity $\approx \frac{.76}{100} C$.

Therefore, relativistic effects are neglected.

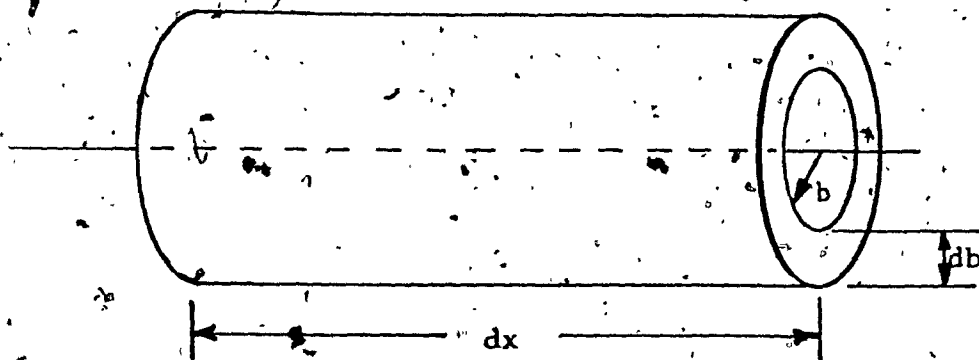
Let us consider Fig I in which

b = distance of an electron from the path of a charged particle



(A)

A particle of charge ze , mass M , and velocity v passes by an electron with an impact parameter b .



(B)

The differential number of electrons with an impact parameter b in the interval db is given by the volume of the cylindrical shell $2\pi b db \cdot dx$.

FIG 1 . Charged particle scattering with electrons.

$Z e$ = charge
 M = mass
 v = velocity

} of the charged particle

The electron is assumed not to move appreciably during the passage of the heavy particle.

The impulse transferred to the electron due to the electric field \vec{E} of the particle is

$$\begin{aligned}
 I_{\perp} &= \int_{-\infty}^{\infty} F_{\perp}(t) dt = e \int_{-\infty}^{\infty} E_{\perp}(t) dt = e \int_{-\infty}^{\infty} E_{\perp}(x) \frac{dt}{dx} dx \\
 &= \frac{e}{v} \int_{-\infty}^{\infty} E_{\perp}(x) dx \quad (2.1)
 \end{aligned}$$

Where only the component of the electric field normal to the particle trajectory have been taken into account. Longitudinal components average to zero when summed from $-\infty$ to ∞ .

From Gauss's law referred to Fig I (b)

$$\begin{aligned}
 4 \pi Z e &= \oint \vec{E} \cdot d\vec{s} = \int_{-\infty}^{\infty} E_{\perp} 2 \pi b dx \\
 \int_{-\infty}^{\infty} E_{\perp} dx &= \frac{2 Z e}{b}, \quad I_{\perp} = \frac{2 Z e^2}{v b}
 \end{aligned}$$

Since the electron was assumed to be at rest, its momentum after the collision $P = I_{\perp}$ and the energy transferred is,

$$E(b) = \frac{P^2}{2m} = \frac{2Z^2 e^4}{mv^2 b^2} \quad (2.2)$$

E is a function of the impact parameter b

From Fig I (b) the number of electrons contained in the cylindrical ring is $N_e 2 \pi b db dx$. N_e is the number of electrons per cm^3 .

$$dE(b) = \frac{4\pi N_e dx Z^2 e^4}{m v^2} \frac{db}{b}$$

$$-\frac{dE}{dx} = \frac{4\pi Z^2 e^4}{m v^2} N_e \ln \left[\frac{b_{\max}}{b_{\min}} \right] \quad (2.3)$$

The finite limits b_{\max} and b_{\min} are imposed by physical considerations.

b_{\max} = distance where the time of passage of the heavy particle's field becomes of the same order as the period of rotation of the atomic electron in its orbit.

$$T = \frac{b}{v} = \frac{1}{\nu} \quad \text{or} \quad b_{\max} = \frac{v}{\nu}$$

b_{\min} = De Broglie wavelength of the electron.

$$b_{\min} = \lambda = \frac{h}{p} = \frac{h}{m v} \quad \text{Then}$$

$$-\frac{dE}{dx} = \frac{4\pi Z^2 e^4}{m v^2} N_e \ln \left[\frac{m v^2}{h \nu} \right] \quad (2.4)$$

The frequencies of the atomic electrons ν are different for each orbit. We replace $\langle h \nu \rangle$ with an average ionization potential \bar{I}

It must be noticed that the mass of the incoming particle does not appear in the stopping power for a heavy particle in a given absorber.

$$-\frac{dE}{dx} = \frac{4\pi Z^2 e^4}{m v^2} N_e \ln \left[\frac{m v^2}{\bar{I}} \right]$$

\bar{I} = constant to be determined experimentally for each element.

This formula is only approximate. Correction due to the screening of K electrons has been derived (Bethe)

2.4 Range of a charged particle:

The range R of a particle is the total length of material the particle will traverse before coming to rest. For $M \gg m$, R is equivalent to the total path x .

$$E = \frac{M v^2}{2}, \quad dE = M v \, dv$$

$$dx = - \frac{M}{Z^2} \frac{m}{4\pi e^4 N e} \frac{v^3 \, dv}{\ln(mv^2/\bar{I})}$$

This equation is not defined for $mv^2 = \bar{I}$ and therefore cannot be integrated over the entire range of the particle. It is mainly employed to describe differences in range $R_2 - R_1$.

In fact the whole theory is not very accurate and not valid for $v \leq c$, Bohr's orbital velocity for the K electron. ¹³⁷ This is the reason why data have been taken from semi empirical values.

At low velocities capture, loss of electrons and nuclear scattering have to be taken into account.

Data: Alpha particles

The values of α stopping power needed for the integration have been calculated with the formula

$$\epsilon_\alpha = \sum_{i=0}^2 a_i E^i$$

ϵ_α = stopping cross section in $\text{eV} / (10^{15} \text{ atoms} / \text{cm}^2)$.

The coefficients a_i are given for H and Ti in reference (3).
 corrections to change the results in $\text{keV} / \text{cm}^2 / \text{g}$ are done
 by multiplying by $\frac{N_A \times 10^{-3}}{W \times 10^{15}} = \frac{6.0226 \times 10^6}{W}$

N_A = Avogadro's number W = atomic weight

For alpha energies between 2000 keV and 4000 keV, where
 few experimental results are available, the determination
 of these coefficients has been done following these steps:

(1) calculation of theoretical values of E_α by the
 Lindhard Winther theory (3)

(2) determination of experimental values using the
 most recent experiments

(3) multiplying the theoretical values by the experi-
 mental to theoretical values ratio for 2000 keV. This
 ratio becomes asymptotic above 1400 keV.

(4) determination of the coefficients a_i by a least
 square polynomial fit

Semi-empirical values are within 5% of the experi-
 mental values (except for Au) at 4000 keV. The use of the
 formula reproduces semi-empirical values to $\pm 2\%$.

Deuterons: The values of the deuteron stopping powers have
 been taken from a least square polynomial fit computed from
 data of ref (4) Energy loss in Ti Tn.

The values of $\frac{dE}{dx}$ in Ti, Tn have been calculated by assuming Bragg's law holds for deuterons and alpha particles. This law states that the energy loss in a compound is the sum of the energy losses in its separate constituents.

Ti Tn

$$\left(\frac{dE}{dx}\right)_{Ti Tn} = \frac{47.9}{47.9 + 3N} \left(\frac{dE}{dx}\right)_{Ti} + \frac{3N}{47.9 + 3N} \left(\frac{dE}{dx}\right)_{T} \quad (2.5)$$

2.5 Interaction of neutrons with matter.

Neutrons have no charge; therefore

(1) They do not lose energy by electromagnetic effects with matter. Interactions due to the neutron magnetic moment are weak and may be neglected.

(2) They are not affected by the coulomb barrier and interact mainly with nuclei.

For 14 MeV neutrons the most probable reactions are

- (1) elastic scattering (n,n) (σ_{el})
- (2) inelastic scattering (n,n') (σ_{in})
- (3) nuclear reactions such as (n,2n), (n,p) and (n, α) reactions (σ_n)

(4) Radiative capture (n, γ), important for thermal neutrons, but becomes very weak for 14 MeV neutrons. In the last case the total cross section σ_t is given $\sigma_t = 2\pi R_a^2$
 $R_a = \text{nuclear radius} \approx 1.5 \times 10^{-13} A^{1/3} \text{ cm}$

This means that σ_t has a value between 1.5 and 6 barns for all elements. σ_n , however is only of the order of millibarns, usually.

TABLE I

DEUTERONS : STATISTICS

Energy (keV)	dE/dx in T (keV/cm)	dE/dx in Ti (keV/cm)	dE/dx in TiTi _{1.35} (keV/cm)	Cross Section (Barn/ster)
200	1.598 x 10 ⁶	3.055 x 10 ⁵	1.853 x 10 ⁶	1.995 x 10 ⁻¹
195	1.569 "	3.060 "	1.847 "	2.106 "
190	1.565 "	3.052 "	1.841 "	2.239 "
185	1.560 "	3.039 "	1.835 "	2.377 "
180	1.551 "	3.026 "	1.827 "	2.512 "
175	1.540 "	3.012 "	1.819 "	2.636 "
170	1.527 "	3.000 "	1.809 "	2.751 "
165	1.513 "	2.989 "	1.799 "	2.857 "
160	1.499 "	2.977 "	1.789 "	2.959 "
155	1.485 "	2.965 "	1.778 "	3.062 "
150	1.471 "	2.951 "	1.767 "	3.170 "
145	1.457 "	2.935 "	1.754 "	3.285 "
140	1.442 "	2.916 "	1.741 "	3.406 "
135	1.427 "	2.894 "	1.727 "	3.532 "
130	1.412 "	2.870 "	1.711 "	3.658 "
125	1.395 "	2.844 "	1.694 "	3.776 "
120	1.378 "	2.814 "	1.676 "	3.879 "
115	1.359 "	2.783 "	1.657 "	3.956 "
110	1.341 "	2.749 "	1.636 "	3.998 "
105	1.322 "	2.713 "	1.614 "	3.995 "
100	1.303 "	2.673 "	1.591 "	3.942 "

TABLE I (cont)

Energy (keV)	dE/dx in T (keV/cm)	dE/dx in Ti (keV/cm)	dE/dx in Ti (keV/cm)	Cross section (barn/ster)
95	1.283×10^6	2.630×10^5	1.566×10^6	3.332×10^{-1}
90	1.262 "	2.583 "	1.539 "	3.663 "
85	1.241 "	2.550 "	1.510 "	3.438 "
80	1.217 "	2.473 "	1.479 "	3.161 "
75	1.195 "	2.400 "	1.444 "	2.842 "
70	1.160 "	2.333 "	1.406 "	2.491 "
65	1.126 "	2.261 "	1.363 "	2.122 "
60	1.033 "	2.177 "	1.306 "	1.751 "
55	1.045 "	2.006 "	1.263 "	1.393 "
50	9.994×10^5	1.939 "	1.210 "	1.062 "
45	9.505 "	1.885 "	1.150 "	7.711×10^{-2}
40	8.995 "	1.775 "	1.087 "	5.277 "
35	8.462 "	1.657 "	1.020 "	3.362 "
30	7.894 "	1.531 "	9.439×10^5	1.959 "
25	7.219 "	1.395 "	8.721 "	1.011 "
20	6.444 "	1.244 "	7.866 "	4.32×10^{-3}
15	5.327 "	1.073 "	6.867 "	1.21 "
10	5.327 "	8.762×10^4	5.634 "	1.0×10^{-4}

CHAPTER IIITHEORETICAL DETERMINATION OF THE NEUTRON YIELD3.1 Target characteristics:

The influence of the target on the neutron flux involves complex problems which include many factors such as target thickness, fabrication procedure, nature of metallic support, age of target, ratio N (N = number of tritium atoms per titanium atom) etc...

The calculation has been done for a thick, new target, mounted on a copper support, with good adhesion and with different ratios N.

Target thickness: The neutron flux increases with the thickness of the target and becomes constant as the target thickness is larger than the path of the incident deuteron. A target with this characteristic is called a "thick target" ($\approx 500 \text{ g / cm}^2$ for a 200 keV accelerator)⁽⁶⁾

Tritium distribution has been considered uniform throughout the target, except at its surface where a thin layer contains almost no tritium. This is due to the superficial oxidation of titanium tritide. It is generally accepted that an incident deuteron loses around 10 keV.

before reaching the given tritium concentration⁽⁵⁾

The degassing rate of the target depends heavily on the manufacturing conditions. For carefully built targets its value does not exceed 1% and becomes zero after 50 to 150 days⁽⁶⁾

The half life of the target is the time the neutron yield takes to decrease to half its original value. The half life of a target for a given energy of incident deuteron is expressed in $\mu\text{A hours cm}^{-2}$ or in coulombs cm^{-2} . It is largely dependent on the density of the target current ($\mu\text{A cm}^{-2}$). Data show large variations and sometimes contradictions⁽⁶⁾ in the given life times.

3.2 Nuclear reactions:

a) Secondary reactions:

- $d(d,n)^3\text{He}$ becomes possible as the drift tube is loaded with deuterium. It has been neglected here because, for a potential below 200 keV, its cross section is 100 times smaller than that of $^3\text{H}(d,n)^4\text{He}$ ⁽⁶⁾

- $^3\text{He}(d,p)^4\text{He}$ is possible because the decay of tritium by β emission results in ^3He . This reaction can be neglected for a new thick target at a potential below 200 keV. It is estimated that, for energies below 200 keV the error contributed by the two reactions is less than 0.3%⁽⁶⁾

b) Reaction ${}^3\text{H} (d,n) {}^4\text{He} + 17.586 \text{ MeV}$.

This reaction is the only source of neutrons considered in this work. For an incident deuteron with energy equal to 200 KeV the Q value 17.586 keV is shared by a 14.206 MeV neutron and an associated 3.58 MeV alpha particle. The neutron yield may be considered isotropic in the C.M. system. The most important characteristic of this reaction is that the cross section is strongly dependent on the energy of the incident particle. The data for these cross sections have been taken from reference⁽⁷⁾ and computed for the different energy values by a least square polynomial fit. These values are tabulated in table (I).

3.3 Method of calculation of neutron flux:

a) Number of tritium atoms / cm^3 .

ρ the density of Ti Tn (g/cm^3) is given by

$$\rho = \frac{47.9 + 3.0 \times N}{47.9} \times 4.54 \times 0.85$$

47.9 = atomic weight of Ti (a.m.u)

3.0 = atomic weight of tritium (a.m.u)

4.54 = density of Ti (g/cm^3)

0.85 = coefficient due to the expansion of titanium lattice during tritiation⁽⁸⁾

RONT, the number of tritium atoms/ cm^3 is therefore

$$RONT = \frac{6.0226 \times 10^{23} \times \rho \times N}{47.9 + (3.0 \times N)}$$

6.0226×10^{23} = Avogadro's number

b) Calculation of stopping power (keV/cm) and range (cm) of deuterons in Ti Tn.

Using formula 2.5 and data from table I, gives the stopping power $\frac{dE}{dx}$ in $\frac{\text{KeV} \cdot \text{cm}^2}{\text{g}}$

$\rho \times \frac{dE}{dx}$ gives stopping power in keV/cm.

The range of the deuterons dx_E is calculated for increments of 5 KeV: $dx_E = (dE \times \frac{dx}{dE}) = 5.0 \times \frac{dx}{dE}$

For each step, the sum of the preceding dx_E gives the distance of the deuteron from the surface of the target. This distance is the path that each alpha particle produced at this step will have to travel before reaching the surface of the target.

c) Probability of a reaction occurring.

The cross section σ for the reaction ${}^3\text{H} (d,n)$ ${}^4\text{He}$ is defined as $\sigma = \frac{\text{flux of reacting deuterons, I}}{\text{flux of incident deuterons per unit area, } I_0}$

The number of tritium atoms is N (atoms/cm³). The probability dP of the reaction taking place in a thickness dx on a target S is

$$dP = \sigma \frac{I/S}{I_0} S n dx = \sigma N dx$$

The probability $P(x)$ for a reaction taking place in a length x where $I(x)$ represents the flux at a distance x into $T_i T_n$ is $dI(x) = dP \cdot I(x) = I(x) \sigma N dx$

$$\frac{dI(x)}{I(x)} = -\sigma N dx$$

$$\ln(I(x)) = -\sigma N x + c \quad \text{at } x=0 \quad \ln(I(0)) = c$$

$$\ln(I(x)) = -\sigma N x + \ln(I(0))$$

$I(x) = I(0) e^{-\sigma N x}$ where $e^{-\sigma N x}$ = probability of survival.

At a distance x , we have $P(x)$ the probability for reacting in x : $P(x) = I - e^{-\sigma N x}$

The following procedure has been followed to calculate the probability of the reaction taking place:

1) The path corresponding to the loss of the 10 first keV has been subtracted

2) The following is step 1: $P(x_1) = I - e^{-\sigma_1 N x_1}$

3) Step 2: $P(x_2) = (1 - e^{-\sigma_2 N x_2}) \times e^{-\sigma_1 N x_1}$

or probability of reaction taking place in step 2 multiplied by probability of survival in step 1.

4) etc... step n $P(x_n) = (1 - e^{-\sigma_n N x_n}) \times e^{-\sigma_{n-1} N x_{n-1}}$

5) The sum of all the probabilities corresponding to each step gives the total probability P of the reaction occurring. For the last step at 10 keV the cross sections at this energy are very small and not accurate. Cross sections below 10 keV have been deleted.

d) Neutron yield: The neutron yield is obtained by multiplying the total probability P , by the number of incident deuterons/sec, I_0 .

e) Determination of deuteron flux I_0 : The accelerator is built to give an energy of $V(\text{keV})$ to a deuteron submitted to a voltage of $V(\text{kV})$.

A current I in mA yields $I \times 10^{-3}$ Coulomb/sec

$$I_0 = \frac{I \times 10^{-3} \times 10^{19}}{1.602} = 6.24 \times 10^{15} \text{ deuterons/sec} \quad \text{or}$$

Results: Program NEUFLU calculates the total probability P and the total neutron flux for different atomic ratios N and different applied voltages V from 200 keV to 10 keV in steps of 5 keV. (Table 2)

TABLE 2

BEAM INTENSITY = 0.8 mA

Deuteron energy (keV)	Number of Tritium atoms/Titanium Atom			
	n=1.7	n=1.8	n=1.9	n=2.0
20	4.65×10^6	4.81×10^6	4.96×10^6	5.10×10^6
30	1.95×10^8	2.01×10^8	2.08×10^8	2.14×10^8
40	1.04×10^9	1.08×10^9	1.11×10^9	1.15×10^9
50	3.17 "	3.29 "	3.40 "	3.50 "
60	7.22 "	7.49 "	7.74 "	7.98 "
70	1.36×10^{10}	1.41×10^{10}	1.46×10^{10}	1.50×10^{10}
80	2.23 "	2.31 "	2.39 "	2.47 "
90	3.30 "	3.42 "	3.54 "	3.66 "
100	4.52 "	4.69 "	4.85 "	5.01 "
110	5.81 "	6.02 "	6.23 "	6.43 "
120	7.09 "	7.36 "	7.61 "	7.86 "
130	8.32 "	8.63 "	8.93 "	9.22 "
140	9.46 "	9.81 "	1.02×10^{11}	1.05×10^{11}
150	1.05×10^{11}	1.09×10^{11}	1.13 "	1.16 "
160	1.15 "	1.19 "	1.23 "	1.27 "
170	1.24 "	1.23 "	1.33 "	1.37 "
180	1.32 "	1.37 "	1.41 "	1.46 "
190	1.39 "	1.44 "	1.49 "	1.54 "
200	1.46 "	1.51 "	1.56 "	1.61 "

NEUTRON FLUX IN NEUTRONS/SECOND

CHAPTER IVEXPERIMENTAL DETERMINATION OF THE NEUTRON FLUX BYALPHA MONITORING4.1 Alpha detection: surface barrier detectors and alpha spectrum.

The interaction of neutrons with matter, briefly exposed in chapter II, accounts for the difficulty of detecting and directly counting the neutrons. But, for each neutron produced by the ${}^3\text{H}(d,n){}^4\text{He}$ reaction, an associated α particle is emitted. The problem is to find a device which can detect α particles with great precision without being perturbed by the "coemitted" neutrons. The silicon surface barrier detectors possess both properties.

The silicon surface barrier detector is formed by an n-type silicon crystal etched with an acid and exposed to the air. The oxidation layer thus formed on the surface has the characteristic of a very thin P-type film. This detector functions as a P-n junction device. The oxidized surface is so thin that it is coated with an evaporated gold film to provide good electrical contact. (Fig 4)

The P barrier is very thin and the incident α particles do not lose much energy in traversing this layer. Practi-

cally all charges due to the ionization of silicon by the particle are formed in the depletion layer and can be transmitted to a charge sensitive preamplifier. The pulse thus determined is transmitted to an amplifier and enlarged sufficiently to be counted by a scaler.

The pulse rise time (10^{-9} to 10^{-8} seconds) and the energy resolution (12 to 13 keV) (9) are considered good performances. In fact, the electronic (devices and not the detector account for most the corrections needed to determine the counting rate.

As the 14 MeV neutrons produce practically no ionization, they are not detected by this device and do not interfere with the counting of α particles.

The energy lost by an alpha particle in the target never exceeds 400 keV (Fig 3). Surface barrier detectors can detect α particles with energies going from 100 keV to 400 MeV. Therefore all α particles can be detected easily by the detector. Thus the system (detector plus electronics) gives an alpha counting rate N_{α} in the solid angle Ω_{α} subtended by the aperture of the α detector. The alpha flux γ_{α} is obtained from N_{α} by following formula:

$$\gamma_{\alpha} = T R_{\alpha} F_g N_{\alpha} \quad \text{where}$$

T = Correction factor due to resolving time and counting statistics.

R_d = Anisotropic correction factor.

F_g = Geometrical correction factor.

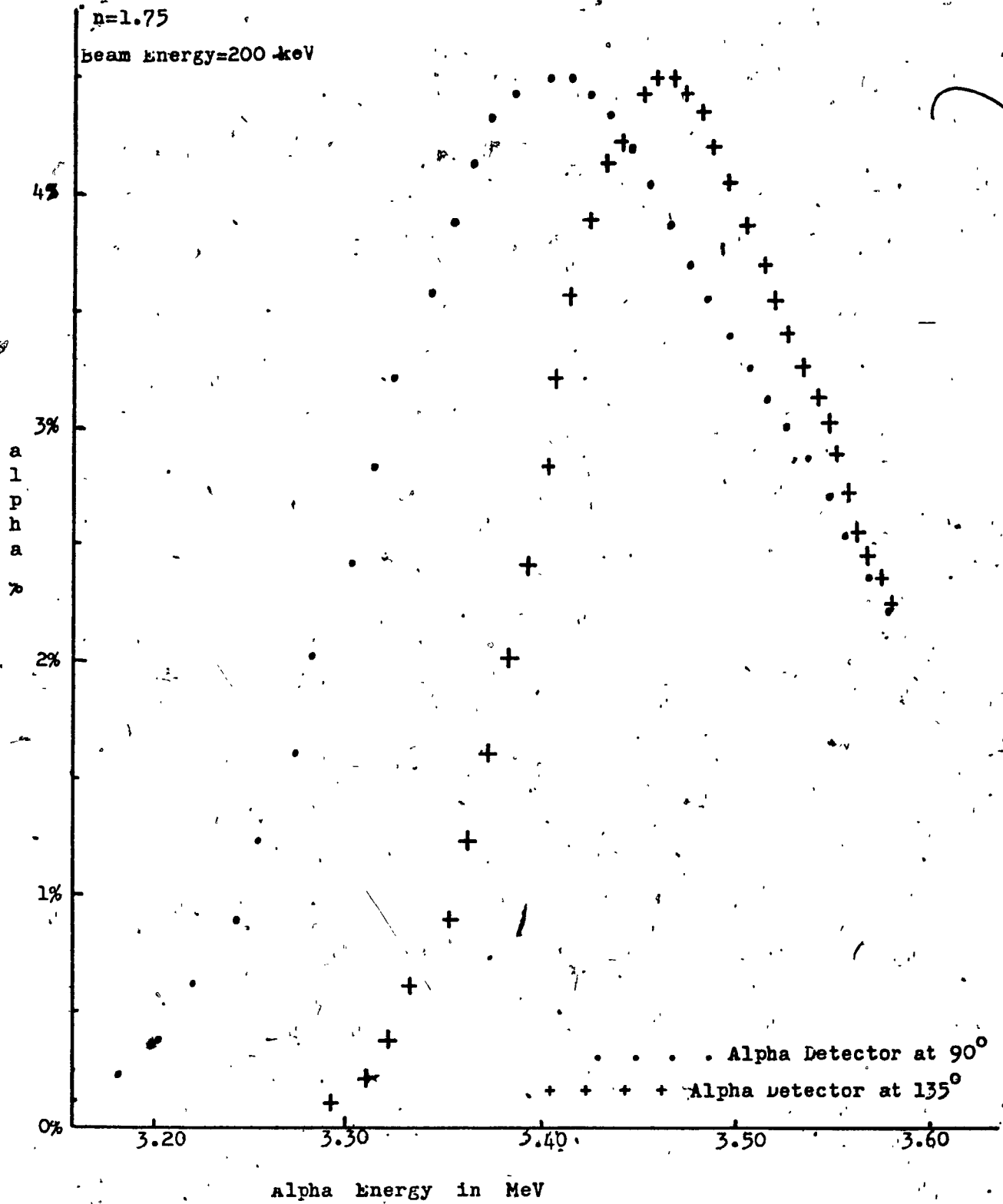


FIG 3 . ENERGY SPECTRUM FOR ALPHA PARTICLES GOING OUT OF THE TARGET.

(computed by program NEUFLU)

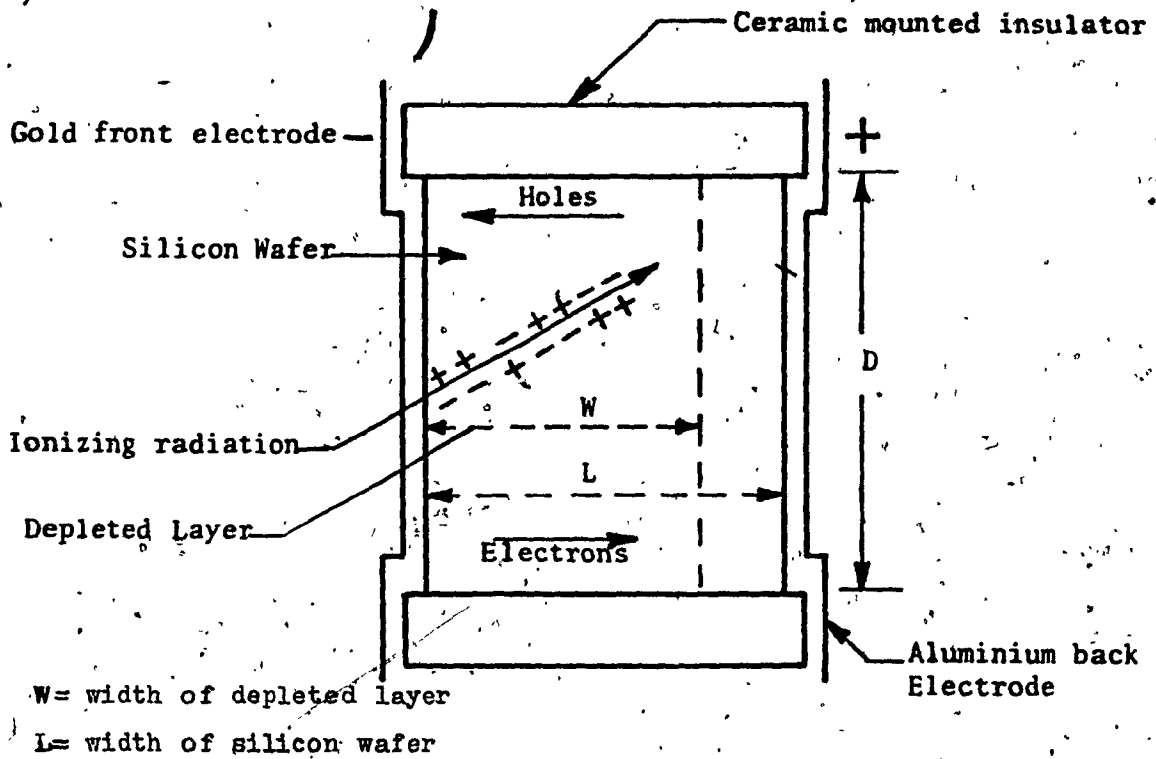


FIG. 4 Schematic of typical surface barrier detector

4.2 CORRECTION DUE TO COUNTING LOSSES:

Resolving time and counting statistics.

If two alpha particles are separated by a shorter period of time than the net resolving time of the whole detection system (detector + preamplifier + amplifier) then, only one will be counted. Since the emission of alpha particles is a random process, each event must be considered as independent of the other and some particles will not be counted, even if the mean count rate is low and the resolving time of the system is short.

It is possible to correct for the counting losses if the dead time per pulse can be determined, provided the correction factor is not too large.

N_o = observed count rate

N = real count rate

t_d = dead time per pulse

1 unit time N_o recorded counts

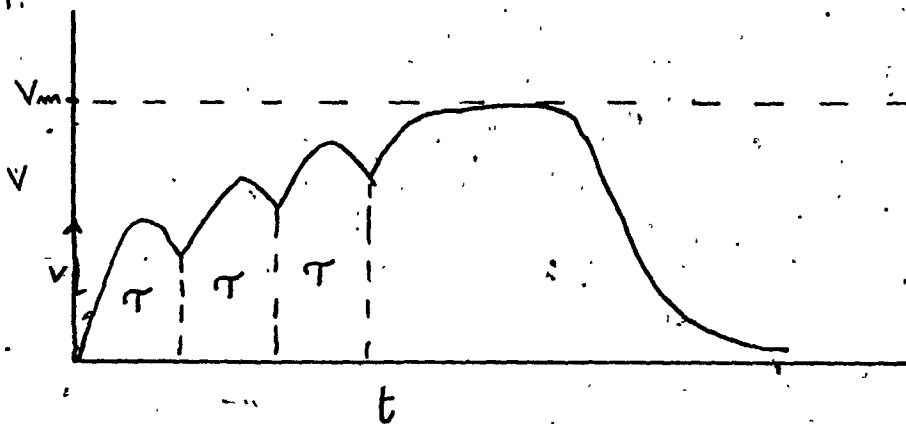
(1 - $N_o t_d$) | $N_o t_d$

The system has been non receptive for a total period $N_o t_d$ and receptive for a time $1 - N_o t_d$. The real count rate N is therefore.

$$N = \frac{N_o}{1 - N_o t_d}$$

This simple formula must be used with caution, because with some detectors, the dead time per pulse is a function of the count rate. To determine the count rate of the system, oscilloscope photographs of amplifier pulses have been taken.

We assume an average time between pulses of τ and a preamplifier maximum output V_m . Then if the average individual pulse height is V , saturation occurs in a time $\frac{V_m}{V} \tau$. Therefore the allowable time between pulses is $\frac{V_m}{V} \tau$. We observed V from oscilloscope photographs and $V_m = 4.5$ volts for the P-10. Sintec pre-amplifier. However we can only get an idea of τ from a few photographs. In fact the counting losses appear to be mainly in the amplifier⁽¹⁰⁾ and no case of preamplifier saturation were observed. However some pulses were too close together for the amplifier to process them, because the amplifier requires 4 μ sec per pulse.



PILE - UP EFFECT

4.3 ANISOTROPIC CORRECTION FACTOR: (5)

Factor $R_\alpha = \frac{P_\alpha(\Omega, C.M.)}{P_\alpha(\Omega, \phi)}$ where

$P_\alpha(\Omega, \phi)$ is the probability that the accelerated deuteron will undergo the reaction and the ensuing α particle will pass through the solid angle whose center is at an angle ϕ with respect to the accelerated deuteron.

$P_\alpha(\Omega, C.M.)$ is the same probability in the center of mass system.

For deuteron energies below 300 keV, the reaction products are practically isotropically distributed

$$P_\alpha(\Omega, C.M.) = R \Omega T \int_0^E \sigma_\alpha(\Omega, C.M.) dE / (dE/dx)$$

$\sigma_\alpha(\Omega, C.M.)$ = differential cross section in barn/steradian.

$$P_\alpha(\Omega, \phi) = R \Omega T \int_0^E \sigma_\alpha(\Omega, \phi) dE / (dE/dx)$$

Where the angle of reference for ϕ ($\phi=0$) is taken as the direction of the accelerated deuteron.

The values for $\sigma_\alpha(\Omega, \phi)$ are calculated from the values published for $\sigma_\alpha(\Omega, C.M.)$ using the following equations.

$$\sigma_\alpha(\Omega, \phi) = [E_\alpha(\phi)] [\sigma_\alpha(\Omega, C.M.)] / \left\{ E_\alpha (A_1 B_1)^{1/2} (B_1/A_1 - \sin^2 \phi)^{1/2} \right\}$$

$$E_\alpha = E_T A_1 \left[\cos \phi + (B_1/A_1 - \sin^2 \phi)^{1/2} \right]^2$$

$$A_1 = \left\{ m_1 M_2 / (M_1 + M_2)^2 \right\} (1 - Q/E_T)$$

$$B_1 = \left\{ m_2 M_1 / (M_1 + M_2)^2 \right\} \left[\left\{ (M_1 + M_2 - m_1) / m_2 \right\} + (m_1 / m_2) (Q / E_T) \right]$$

E_T = Available energy $Q + E_d$ $Q = + 17.589$ MeV

E_d = Kinetic energy of deuteron E = kinetic energy of α

ϕ = Laboratory angle of α detector

M_1 = Mass of neutron M_2 = mass of ${}^4\text{He}$

m_1 = Mass of ${}^2\text{H}$ m_2 = mass of ${}^3\text{H}$

Ref(5) shows that for the α detector located at 90°

$R_\alpha = 1.0035$ for $E_d = 105$ keV

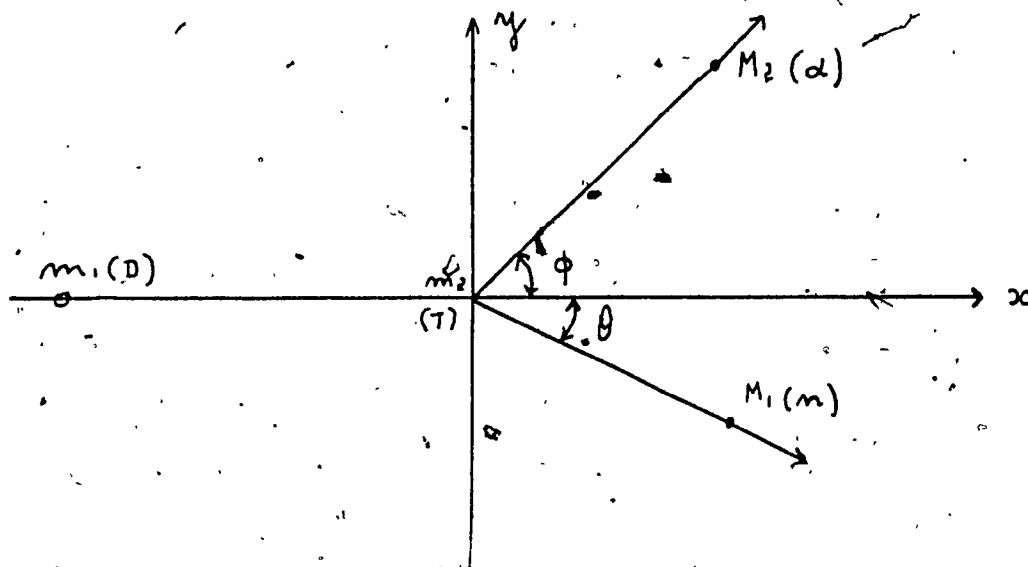
$R_\alpha = 1.0055$ for $E_d = 205$ keV

For the α detector located at 135° ,

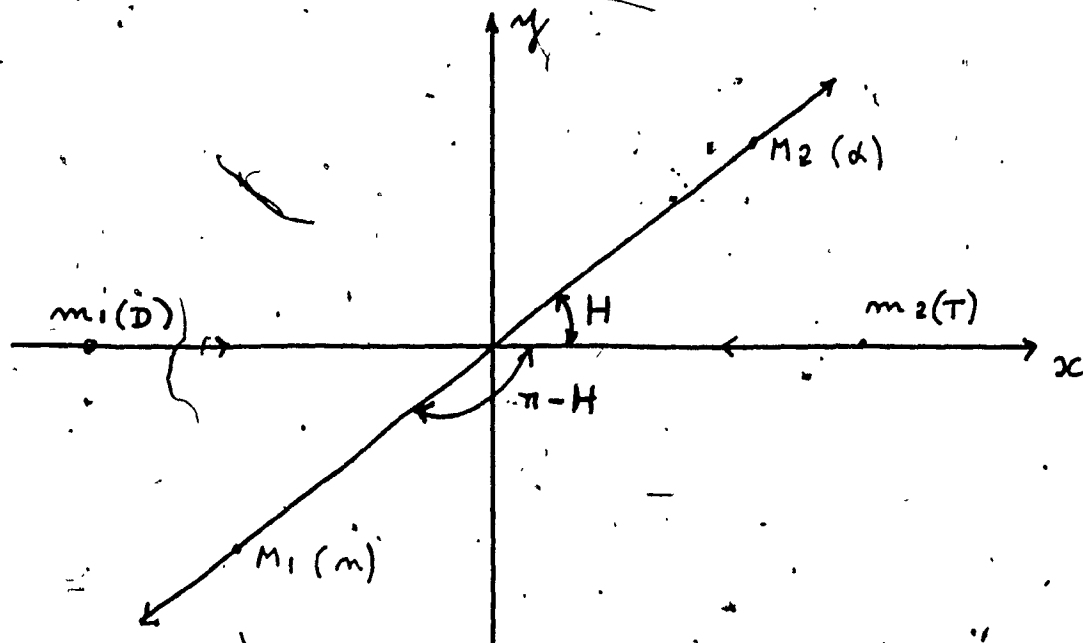
$R_\alpha = 1.1305$ for $E_d = 105$ keV

$R_\alpha = 1.1638$ for $E_d = 195$ keV

If the R_α can be neglected for the 90° detector it has to be taken into account for the α detector located at 135° .



(a) LABORATORY COORDINATES



(b) C.M. COORDINATES

Fig 2 - particle nuclear reaction with emission of two different particles

4.4

GEOMETRICAL FACTOR

The geometrical factor F_g is calculated for a point source located on the central axis of the beam⁽⁵⁾ In that case the total flux is distributed over the whole sphere of 4π ster. If the detector subtends an angle Ω or the geometrical factor $F_g = \frac{4\pi}{\Omega}$.

By definition $\Omega = \frac{A}{R^2}$ where A is the spherical area subtended by a detector aperture and R is the distance from the center of the target to the center of a detector aperture, From Fig 6

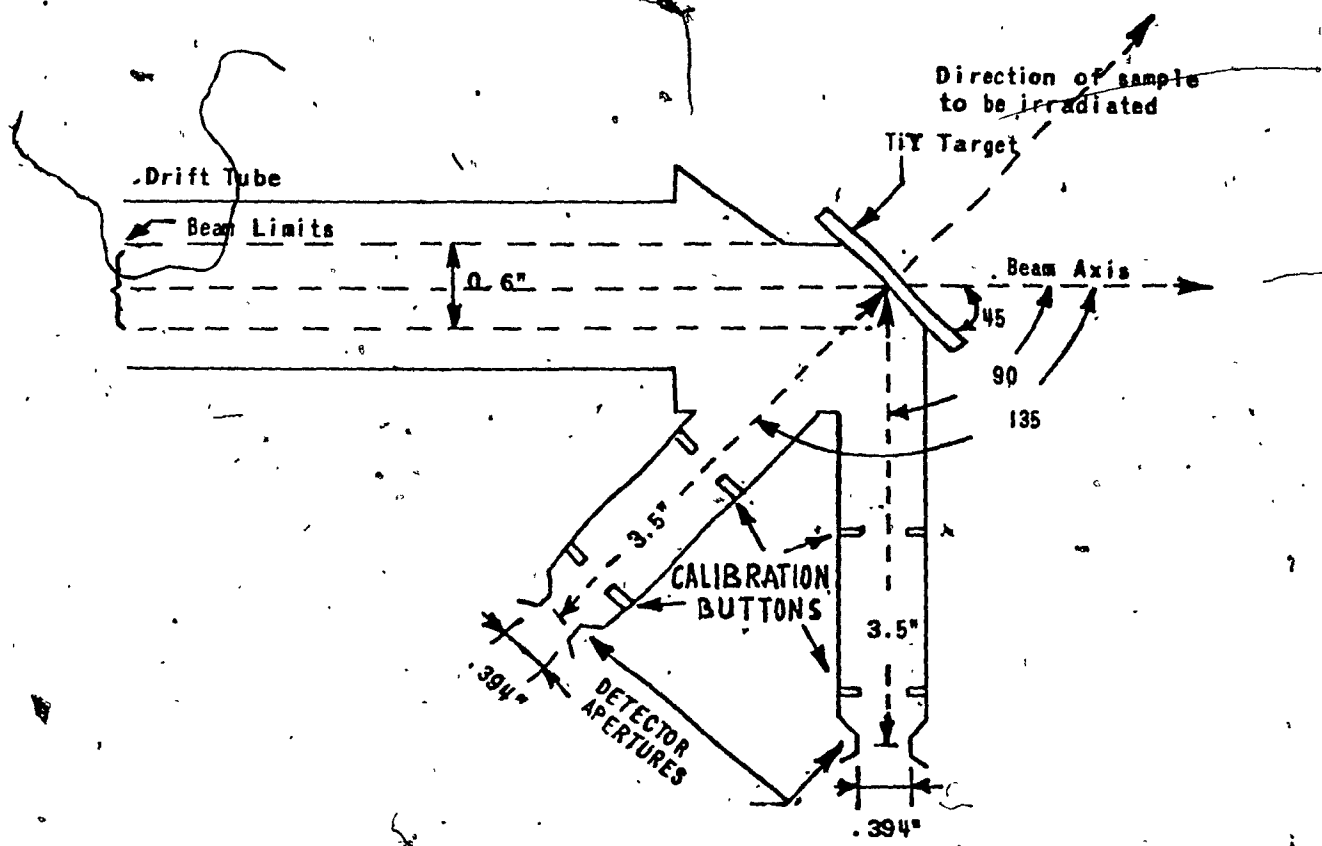


FIG. 5 TARGET ASSEMBLY DESIGN

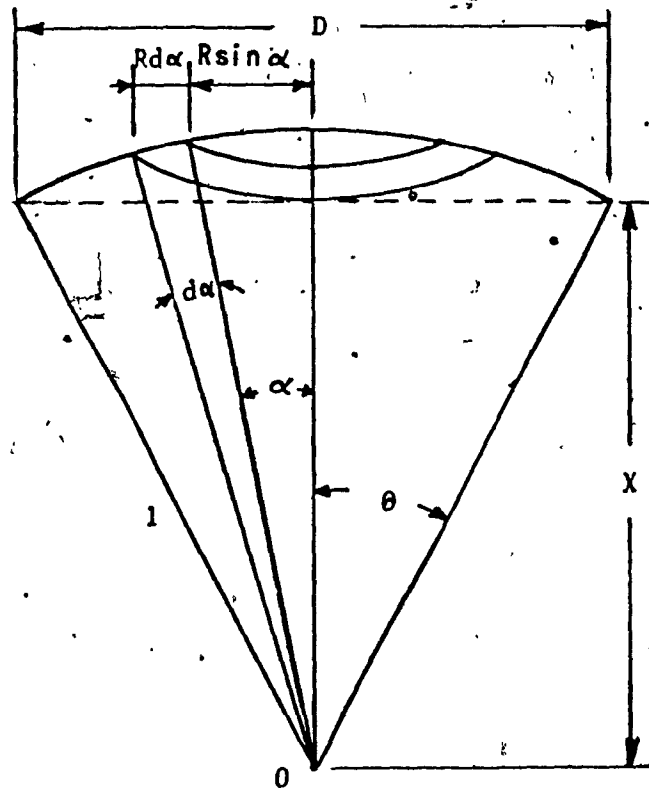


FIG. 6 Geometry of a point source located on the center axis of a circular aperture.

$a = D/2$
 $q = x$
 $R = R - x$

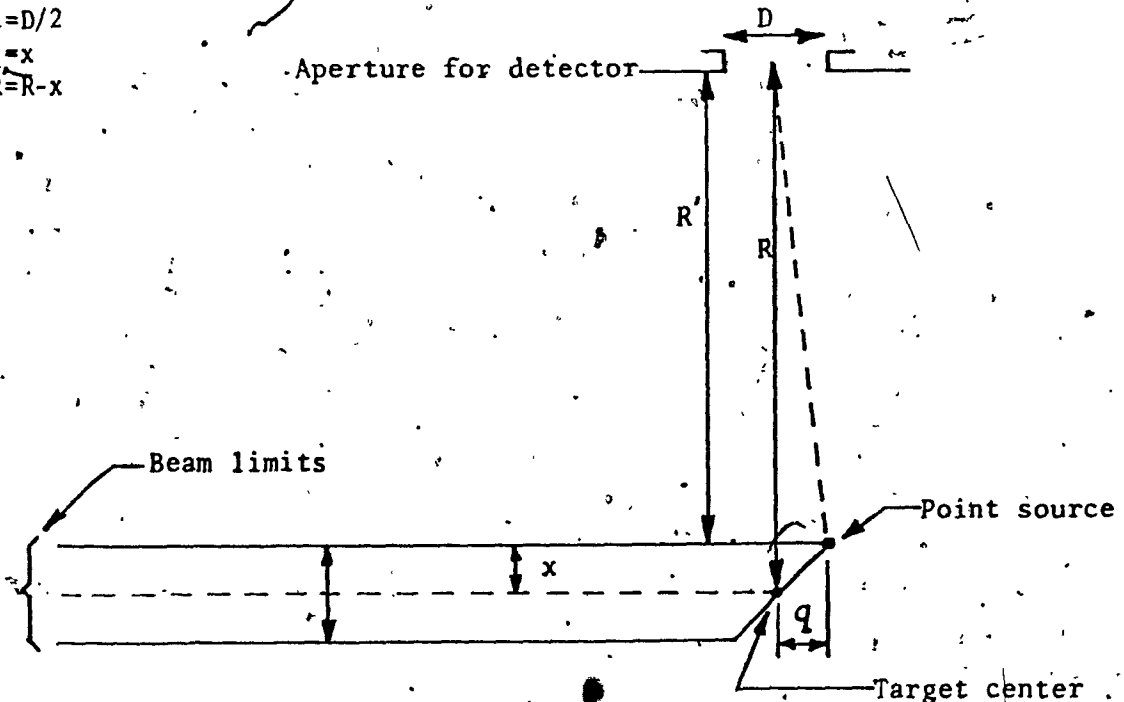


FIG. 7 Worst possible geometry condition for a point source located off target center.

$$A = 2\pi R^2 \int_0^\theta \sin \alpha \, d\alpha = 2\pi R^2 \left[-\cos \alpha \right]_0^\theta$$

$$A = 2\pi R^2 (1 - \cos \theta) \quad \Omega = 2\pi (1 - \cos \theta)$$

$$F_g = \frac{2}{1 - \cos \theta}$$

The calculation can be done using tables of ref.

or by the use of the formula

$$\Omega = \pi \left\{ z^{-2} - \frac{3}{4} (1 + 2\rho^2) z^{-4} + \frac{5}{8} (1 + 6\rho^2 + 3\rho^4) z^{-6} \right\} \quad 4.1$$

Where $z = \frac{R'}{a}$ $\rho = \frac{q}{a}$

a = radius of α detector aperture

R' = distance one must extend the center axis of the aperture before he can draw a line perpendicular to the axis and intersecting the point source.

q = distance of the point source to a line which represents the center axis of the aperture.

For the accelerator used at Concordia University

$$R = 3.5'' \quad a = 0.197'' \quad x = \frac{1''}{16}$$

calculation using equation 4.1

1) Beam centered: detector at 90° , 135°

$$R' = R = 3.5'' \quad a = 0.197'' \quad q = 0, p=0, z = \frac{3.5}{.197} = 17.78$$

$$\Omega = .003156 \pi$$

$$F_g = \frac{4\pi}{\Omega} = 1267$$

2) Beam not centered

a) beam high for detector at 90° (Fig 7)

R' = R - x = 3.4375" a = 0.197" x = q = .0625"

Z = 17.45 p = q/a = .317

Ω = .0032745 π

Fg = 4π/Ω = 1222 maximum % error = ± 3.7 %

detector at 135°

R' = R = 3.5" a = 0.197" q = x/2 = 0.0884"

Z = 17.78 p = .449

Ω = .003153 π

Fg = 4π/Ω = 1269 maximum % error = 0.16%

The results show that the detector located at 90° is the most concerned by an error in focusing the beam.

For a beam off center by 1/16" the percentage error is around 3.7 % for the detector located at 90°. The detector located at 135° yields an error of .2% approximatively.

In fact the beam is not a point source and when it is out of focus, a part of it does not hit the target, thus reducing the counting rate.

4.5
DETERMINATION OF THE LOSSES DUE TO A MISFOCUSED BEAM

Radius of beam = 0.3" out of center by $\frac{1}{16}$ " (Fig 8)

- Equation of circle $x^2 + (y - .0625)^2 = .09$
 or $x^2 + y^2 - .125y - .0861 = 0$

- Equation of ellipse $\frac{x^2}{2 \times .09} + \frac{y^2}{.09} = 1$ or $x^2 + 2y^2 = 0.18$

The resolution of the system formed by the two equations yields $P_1 (0.2340, 0.2502)$, $P_2 (-0.2340, 0.2502)$

The shaded area represents the part of the beam which does not reach the target = A lost

A lost = Area of circular segment P_1P_2 - Area of elliptical segment P_1P_2 .

1) Area of circular segment:

This area is the same that the area of the corresponding circular segment of the same circle with center at the origin = $2 \int_{(.2502 - 0.0625)}^{0.3} (.09 - y^2)^{\frac{1}{2}} dy$

$$= 2 \times \frac{1}{2} \left[y (.09 - y^2)^{\frac{1}{2}} + .09 \sin^{-1} \frac{y}{1.31} \right]_{.1877}^{0.3} = .03663$$

2) Area of elliptical segment:

$$= 2 \int_{.2502}^{0.3} 2 (.09 - y^2)^{\frac{1}{2}} dy = \frac{2 \times 2}{2} \left[y (.09 - y^2)^{\frac{1}{2}} + .09 \sin^{-1} \frac{y}{1.31} \right]_{.2502}^{.3} = .01585$$

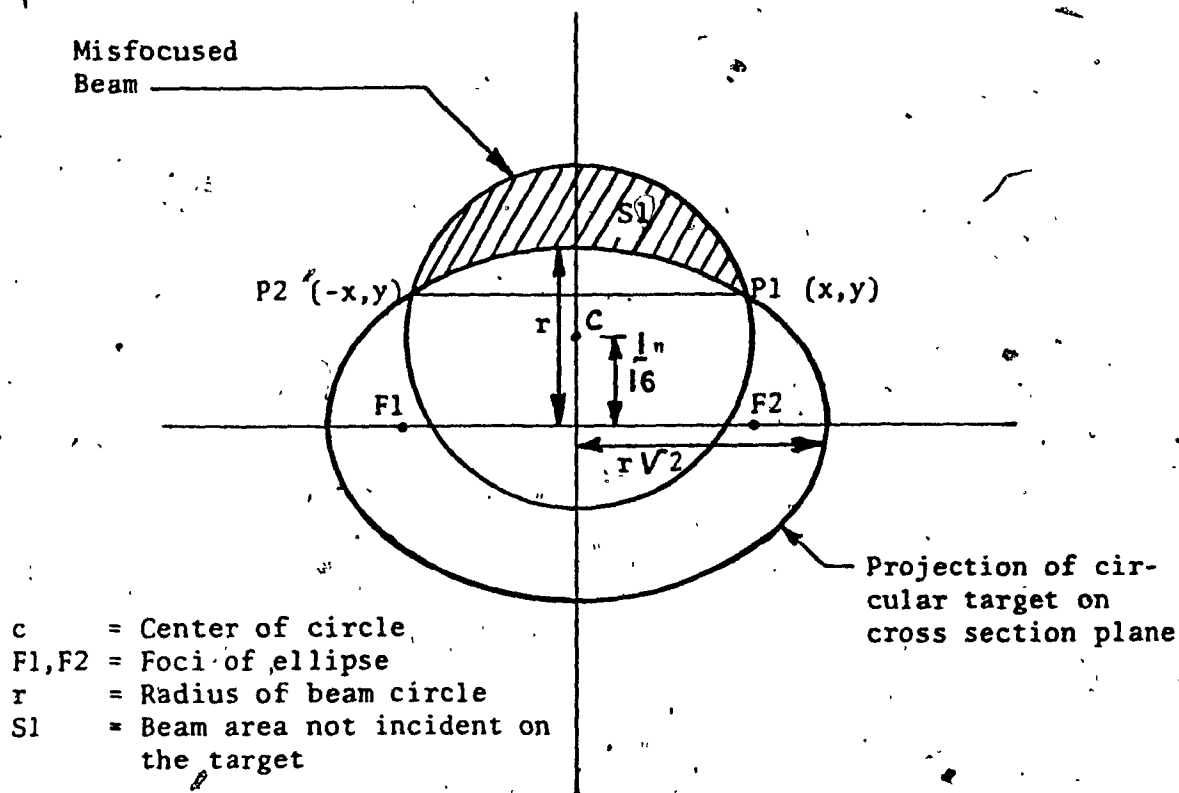


FIG. 8 = Cross section of Beam normal to its direction
 Beam out of focus by $\frac{1}{16}$ "

$$A \text{ lost} = .03663 - .01585 = .02078$$

Which represents 7.35% of the surface of the beam

A good calibration is very important, if an error of

$\frac{1}{16}$ of an inch gives 7.35% of beam out of the target,
 an error of .15" ($\frac{1}{2}$ of the radius) gives a loss of 22.8%
 of the beam.

4.6 EXPERIMENTAL RESULTS AND CALCULATIONS:

An experiment has been performed using the Concordia University neutrons accelerator and measurement were made using

- 1) one alpha detector located at 90°
- 2) a 2.5cm copper foil located at 3.6cm perpendicular to the target axis; irradiation time was 20 min.

1) Alpha detector results:

The total number of counts = 20,047,969 counts which gives 16707 counts/sec.

Correction for losses due to time delay in electronic system.

$$N = \frac{N_0}{1 - N_0 t_d} = \frac{1.6707 \times 10^4}{1 - 1.6707 \times 10^4 \times 4 \times 10^{-6}} = 1.790 \times 10^4 \text{ counts/sec.}$$

Correction for geometrical factor F_g

$$\text{Neutron flux} = N F_g = 1.790 \times 10^4 \times 1.267 =$$

$$\text{Neutron flux} = 2.27 \times 10^7 \text{ Neutron/sec}$$

4.7 FOIL ACTIVATION TECHNIQUE FOR MEASURING NEUTRON YIELD

A copper foil placed at 3.6cm from the target is irradiated for 20 minutes during which the characteristic reaction $\text{Cu}^{63}(n, 2\gamma)\text{Cu}^{62}$ takes place. Then, after one minute of cooling, the 0.51 MeV gamma rays emitted from positron annihilation as Cu^{62} decays into Ni^{62} are counted for one minute at 3cm from a 3" Na I detector. From the number of counts obtained (3133) the neutron flux is determined according to the following steps:

1) Determination of total number of activated copper atoms N_a with respect to the neutron flux Φ

The efficiency of the reaction $\tau = \tau_{AV}$

$\sigma =$ cross section in $\text{cm}^2 = .53 \times 10^{-24}$

$n =$ total number of Cu^{63} atoms

$n = \frac{\text{Weight of foil} \times \text{Avogadro's number} \times \% \text{ of } \text{Cu}^{63} \text{ in copper}}{\text{Atomic Weight of Cu}}$

Atomic Weight of Cu

$$\tau_{AV} = \frac{1.2892 \times 6.02 \times 10^{23} \times .691 \times .53 \times 10^{-24}}{63.54} = 0.0447$$

The total efficiency ($\tau_{AV} \times$ geometrical efficiency) has been evaluated using program NADISC for a:

source of radius = 0.762cm (target)

distance, foil target = 3.6cm

radius of foil = 1.25cm

thickness of foil = 0.025cm.

Total efficiency = 3.0995×10^{-5}

$N_a = \text{total efficiency} \times (1 - e^{-\lambda t_i}) t_i \times Y$

$t_i(1 - e^{-\lambda t_i}) = \text{correction for time irradiation } t_i$

$\lambda = 0.0701 \text{ min}^{-1}$ (half life of $\text{Cu}^{62} = 9.9 \text{ min.}$)

$$N_a = 3.0995 \times 1200 \times .754 Y \times 10^{-5} = 2.804 \times 10^{-2} Y$$

2) When counting the gamma rays, the relation between the disintegration rate of the source at zero decay N_0 and the count per minute at zero decay N_p is

$$N_0 = N_p \times 8.703 \quad (10)$$

Using the same conditions as Wood in (reference 10) we are allowed to use the same correction factor for geometry, absorption in lucite and can, branching ratio and photopeak efficiency.

$$N_0 = \lambda N_a$$

$$N_p = \frac{.0701 \times 2.804 \times 10^{-2}}{8.703} = 2.26 \times 10^{-4} Y$$

3) The window count corrected for back ground $C_w = 58.353 - .220 = 58.133$ count/min. and average decay time ($t_d = 1 \text{ min.}$) is related to the neutron yield by

$$N_p = C_w e^{\lambda t_d}$$

$$Y = C_w \times 1.073$$

$$Y = \frac{58.133 \times 1.073}{2.26 \times 10^{-4}} = 2.76 \times 10^8 \text{ N/s}$$

CONCLUSION

In this work, the determination of the 14Me V neutron yield of a Ti T target bombarded by deuterons has been done theoretically and experimentally.

Theoretically, the main difficulties encountered have been the determination of the best data to be chosen for the calculations and the approximations to be done.

The difference between the stopping power of deuterons in titanium varies greatly between experimental and theoretical data, and even between experimental data differences of 30% have been found.

The main approximations are :

- The use of Bragg's law for energy lost in a compound.

This rule is not completely reliable.⁽³⁾

- The uniformity of tritium distribution under the surface layer where oxidation takes place.

Our calculation is valid only for a target which has not been used before. The differences in values encountered among different authors as far as the half life of a target is concerned did not allow us for correction due to the total irradiation time of the target.⁽⁶⁾ This fact explains that no experimental verification of our theoretical calculation was possible with our old target.

In spite of all these approximations and differences in data our calculated neutron yields are 7.5% lower than those of

reference (8) and 8.7% higher than those of reference (6) in the same conditions of voltages and ratios N.

The evaluation of the alpha counting technique shows that there is no loss of alpha particles due to energy losses in the target and that the best target assembly design is represented by:

- a) An alpha detector at 90° from the beam. This detector is practically insensitive to the errors due to the anisotropic factor (App. I)
- b) An alpha detector at 135° from the beam. This detector is practically insensitive to errors due to the geometrical factor.

The comparison between the neutron yield measured by the alpha monitoring and foil activation techniques are explained by the difference in the dimensions of the diameters of the calibrating buttons.

A difference of 60% to 100% was expected. The main explanations for it are: mislocation of the foil (an error of 2mm in position yields a 10% difference in the neutron flux). Difficulties due to the unexpected stopping of the machine during the experiment and the difficulties in keeping the deuteron flux constant are the others causes.

But a difference of one order of magnitude between both results is explained by a difference in the dimensions

of the diameter of the calibrating buttons.

These new dimensions, discovered just at the end of the experiment, need a completely different approach than the point source or disc source used to determine the geometrical factor.

APPENDIX I

Error in R_α due to the composition of the beam. (5)

The determination of R_α has been done for a 100% $D1^+$ beam of deuterons. In fact this assumption may contribute to a serious error in the calculation. The beam is composed of $D1^+$, $D2^+$, $D3^+$. The percentage of each ion varies with the conditions of experiment and does not always follow the specification of the ion source. Upon entering the target, the $D2^+$ will dissociate into two $D1^+$ and the $D3^+$ into 3 $D1^+$ having kinetic energies which correspond to $\frac{1}{2}$ and $\frac{1}{3}$ of their primitive energy E .

If the beam composition is known, the value of R_α corresponding to these conditions can be calculated according to the formula

$$R_\alpha = \frac{[(\% D_1^+)/Z] X(E) + 2[(\% D_2^+)/Z] X(\frac{E}{2}) + 3[(\% D_3^+)/Z] X(\frac{E}{3})}{[(\% D_1^+)/Z] Y(E) + 2[(\% D_2^+)/Z] Y(\frac{E}{2}) + 3[(\% D_3^+)/Z] Y(\frac{E}{3})}$$

Where X is the evaluation of $P_\alpha(\Omega, CM)$

Y is the evaluation of $P_\alpha(\Omega, \phi)$.

$E, \frac{1}{2}E, \frac{1}{3}E$, represent the end point energies at which the above functions are evaluated.

Z represents the total number of ions in the beam.

$$Z = \% D1^+ + 2(\% D2^+) + 3(\% D3^+)$$

For an accelerating potential of 150kV, the difference for R between a 100% $D1^+$ beam and a 31.1% $D1^+$, 66.7% $D2^+$ and 2.2% $D3^+$ beam is:

1.7% for the α detector located at 135° .

Practically 0 for the α detector located at 90° . (5)

The α detector located at 90° shows practically no variation for various beam compositions.

APPENDIX II

```

PROGRAM NEUFLU(TAFE1,TAPE2,TAPE3,TAPE4,
+TAFES,TAPE6,OUTPUT)
*THIS PROGRAM COMPUTES THE NEUTRON FLUX OF
*TIT TARGET AND THE ENERGY OF ALPHA PARTICLES
*GOING OUT OF THE TARGET
*
*
*
*NAME OF PARAMETERS
*BNT=NUMBER OF TRITIUM ATOMS/TITANIUM ATOM
*SCIA=CURRENT INTENSITY IN AMPERES
*KENER=ENERGY OF DEUTERON BEAM
*
CALL GET(SHTAFE1,5HBKEV1,0,0)
CALL GET(SHTAFE2,6HBDEST1,0,0)
CALL GET(SHTAFE3,6HBDESTR,0,0)
CALL GET(SHTAFE4,7HBCROSEC,0,0)
CALL GET(SHTAFES,6HBALST1,0,0)
CALL GET(SHTAFE6,6HBALSTR,0,0)
BNT=1.4
SCIA=.001
KENER=1.45
*
*CALCULATION OF NUMBER OF TRITIUM ATOMS
*FER CC
*
*
RO=(47.9+3.*BNT)*4.54*0.85747.9
RONT=BNT*RO*6.025E+23/(47.9+3.*BNT)
PRINT 110,RO,RONT
110 FORMAT(3HRO=,F5.3,4HG/CC,5X,6HRONT=,E9.4,
+15HTRITIUM.ATOM/CC)
*
*CALCULATION OF DEUTERON STOFFING POWER IN
*TIT AND NEUTRON FLUX
*
DIMENSION BEN(39),BSTI(39),BSTR(39),BSTF(39),
+BSTFCM(39),DX(39),SUM(39),BFROT(39),
+SFROT(39),BFROS(39),BCRO(39),SUMFRO(39)
PRINT 210
210 FORMAT(8HBEN(KEV),1X,14HBSTFCM(KEV/CM),
+2X,6HDX(CM),3X,7HSUM(CM),6X,5HBFROS)
READ(2,220)(BSTI(1),I=1,39)
220 FORMAT(6X,E10.5)
READ(3,230)(BSTR(1),I=1,39)
230 FORMAT(6X,E10.5)
READ(1,215)(BEN(1),I=1,39)
215 FORMAT(6X,13)
READ(4,240)(BCRO(1),I=1,39)
240 FORMAT(6X,E10.5)

```

```

N=41-KENER/5
SUM(N)=0.
DO 250 K=N,39
  BSTF(K)=(47.9*BSTI(K)+3.*BNT*BSTR(K))/
  +(47.9+3.*BNT)
  BSTFCM(K)=BSTF(K)*RO
  DX(K)=5./BSTFCM(K)
  SUM(K)=SUM(K-1)+DX(K-1)
  IF(K.LT.N+2)GO TO 250
  SPROT(N+1)=1.
  BFROT(K)=1./EXP(RONT*DX(K)*BCRO(K)*3.14*4.)
  SFROT(K)=SFROT(K-1)*BFROT(K)
  BFROS(K)=SPROT(K-1)*(1.-BFROT(K))
  IF(K.LT.38)GO TO 1
  PRINT 280,(BEN(K),BSTFCM(K),DX(K),SUM(K)
  +,BFROS(K))
  280 FORMAT(13,4X,E10.4,3X,E10.4,1X,E10.4,
  +1X,E15.9)
  1 SUMFRO(N+1)=0.
  SUMFRO(K)=SUMFRO(K-1)+BFROS(K)
  FLUX=SCIA*SUMFRO(K)*1.0E+19/1.602
  IF (K-39.EQ.0) GO TO 290
  250 CONTINUE
  290 PRINT 291,(SUMFRO(K))
  291 FORMAT(18HTOTAL PROBABILITY=,E13.7)
  PRINT 295,(FLUX)
  295 FORMAT(13HNEUTRON FLUX=,E13.7)
*
*CALCULATION OF ALPHA STOFFING FOWER IN
*TITANIUM TRITIDE
*
  DIMENSION ASTI(100),ASTR(100),ASTF(100),
  +ASTFCM(100),DA(100),ASU(100)
  PRINT 350
  350 FORMAT(14HASTFCM(KEV/CM),2X,
  +6HDA(CM),5X,7HASU(CM))
  READ(5,310)(ASTI(J),J=1,100)
  310 FORMAT(6X,E10.5)
  READ(6,320)(ASTR(J),J=1,100)
  320 FORMAT(6X,E10.5)
  DO 330,J=1,100
  ASTF(J)=(47.9*ASTI(J)+BNT*3.*ASTR(J))/
  +(47.9+3.*BNT)
  ASTFCM(J)=ASTF(J)*RO
  DA(J)=10./ASTFCM(J)
  ASU(1)=0.
  ASU(J)=ASU(J-1)+DA(J)
  IF(J.LT.99)GO TO 330
  PRINT 340,(ASTFCM(J),DA(J),ASU(J))
  340 FORMAT(E10.4,5X,E10.4,2X,E10.4)

```

330 CONTINUE

*
*CALCULATION OF ENERGY OF ALPHA PARTICLE
*WHEN GOING OUT OF THE TARGET

*
DIMENSION AENER(39),FADIF(3900)
FRINT 410
410 FORMAT(9HDEUTENER,5X,9HALFHA 90 ,
+6X,9HALFHA 135)
DO 420 M=N,39
DO 430 L=1,100
FADIF(L)=SUM(M)-ASU(L)
IF (FADIF(L))421,421,430
430 CONTINUE
421 AENER(M)=3590.-10.*L
IF(M.LT.39)GO TO 420
DIMENSION SAENER(39),SFADIF(100)
DO 435 I=1,100
SFADIF(I)=SUM(M)/SQRT(2.)-ASU(I)
IF (SFADIF(I))436,436,435
435 CONTINUE
436 SAENER(M)=3590.-10.*I
IF(M.LT.39)GO TO 420
PRINT 437,(HEN(M),AENER(M),SAENER(M))
437 FORMAT(2X,13,6X,E9.4,6X,E9.4)
420 CONTINUE
STOP
END

REFERENCES

- 1) D. de Soete, R. Gijbels, J. Hoste, Neutron Activation Analysis. Wiley interscience, 1972.
- 2) Melissinos, Experiments in Modern Physics; New-York: Academic Press, 1967.
- 3) J.F. Ziegler and W.K.ohn ⁴He Stopping and Backscattering: Atomic Data and Nuclear Data. Tables; Vol.13, No 5, May 1974.
- 4) L.C Northcliffe and R.F Schilling; Range and Stopping Power Tables for Heavy Ions. Nuclear Data Tables; A7; (233-463) 1970.
- 5) T.R. Fewel. An Evaluation of the Alpha counting Technique for determining 14MeV Neutrons Yields; Nuclear Instruments and Methods 61 (1968).
- 6) M. Guillaume, G. Delfiore, G. Weber and M. Cuypers LA TR 71.60. On the 14 MeV Neutron producing Tritiated Titanium Targets, Part II Study of the Mechanisms of Behavior and Neutron Yields.
- 7) H. Liskien and A. Paulsen. Neutron Production Cross Sections and Energies for the Reactions $T(p, n)^3\text{He}$, $D(d, n)^3\text{He}$, $T(d, n)^4\text{He}$ Nuclear Data Tables. Vol. 11, No. 7, June 1973
- 8) E.M. Gunnerson and G. James; On the Efficiency of the Reaction $^3\text{H}(d, n)^4\text{He}$ in Titanium Tritide bombarded with Deuterons; Nuclear Instruments and Methods 8, 1960 (173-184)
- 9) Ortec Laboratory Manual. A. Semi Conductor Detectors and Associated Electronics.
- 10) Pulse Pile-up in Preamplifiers, Misconceptions and Facts. Tennelec Tech . Vol 3, No 1, jan 74.

11) D.E. Wood; Texas Convention for Measuring Neutron output;
Technical Bulletin; Karman Nuclear.